




Article

On the Performance of LDPC-Coded Large Intelligent Antenna System

Ali Gashtasbi ¹, Mário Marques da Silva ^{2,3,4,5,*} , Rui Dinis ^{1,3,4}  and João Guerreiro ^{1,3,4} 

¹ Faculty of Sciences and Technology, Universidade Nova, 2829-516 Caparica, Portugal
² Department of Engineering and Computer Sciences, Universidade Autónoma de Lisboa, 1169-023 Lisboa, Portugal
³ Autonomia TechLab, 1169-023 Lisboa, Portugal
⁴ Instituto de Telecomunicações, 1049-001 Lisboa, Portugal
⁵ Ci2—Centro de Investigação em Cidades Inteligentes, 2300-313 Tomar, Portugal
* Correspondence: mmsilva@autonomia.pt

Abstract: This article studies Large Intelligent Systems (LIS) along with Single Carrier with Frequency Domain Equalization (SC-FDE), utilizing Low-Density Parity-Check (LDPC). Four different receivers are studied in the scenarios described above, namely Equal Gain Combining (EGC), Maximum Ratio Combining (MRC), Zero Forcing (ZF), and Minimum Mean Squared Error (MMSE). The results of this article show that the use of LDPC codes leads to an improvement of performance by about 2 dB for a 4X25 LIS system and by 3 dB for a 4X225 LIS system, as compared to similar systems without LDPC codes. Moreover, for all simulations, the MMSE receiver achieves the best overall performance, while EGC performs the worst.

Keywords: 6G; LDPC; LIS systems; SC-FDE



Citation: Gashtasbi, A.; da Silva, M.M.; Dinis, R.; Guerreiro, J. On the Performance of LDPC-Coded Large Intelligent Antenna System. *Appl. Sci.* **2023**, *13*, 4738. <https://doi.org/10.3390/app13084738>

Academic Editors: Christos Bouras and Junseop Lee

Received: 14 December 2022

Revised: 19 February 2023

Accepted: 7 April 2023

Published: 10 April 2023



Copyright: © 2023 by the authors. Licensee MDPI, Basel, Switzerland. This article is an open access article distributed under the terms and conditions of the Creative Commons Attribution (CC BY) license (<https://creativecommons.org/licenses/by/4.0/>).

1. Introduction

1.1. Motivation

The future of communications is going to become intelligent and interactive as it tries to make human-made surfaces electronically active, improving wireless communication. In this regard, the emergence of the Internet of Things (IoT) and billions of terminals that require access to wireless communications have made researchers put a lot of effort into solving communication problems [1]. m-MIMO (Massive MIMO—Multiple Input Multiple Output), UM-MIMO (Ultra Massive-MIMO), and ELAA (Extremely Large Antenna Arrays) are three of the most significant developments in communication system design in recent decades, and they have significantly improved data rate, network capacity, and performance. In this regard, the LIS concept can be viewed as a beyond-massive MIMO in a telecommunications network with increased capacity and data rate, where the number of antennas is even higher.

Traditionally, wireless communications are established in the far-field, that is, with propagation distances beyond the Fraunhofer distance (the Fraunhofer distance is only a few wavelengths). The LIS system comprises several panels, and each panel includes several antenna elements. The LIS system acts as a near-field beamforming; that is, the communication is established behind the Fraunhofer distance [2,3]. In this case, the individual array elements are in the far-field but not the array as a whole. Consequently, the focus is established not only in the bearing and elevation planes but also in the distance dimension. This allows for the reduction of interferences between users that are aligned but located at different ranges, bringing another advantage, as compared to traditional beamforming. The typical distance between the antenna elements is $\lambda/2$. The channel correlation between the antenna elements allows for the creation of the above-described beam.

A block transmission strategy has already been presented. Single carrier with frequency domain equalization [4,5] is also discussed and analyzed in this article, but it is applied to the Large Intelligent Surface (LIS). Furthermore, this paper analyzes the use of Low-Density Parity-Check (LDPC) codes to this combined system. Training sequences are used in this article to make the results more realistic. There are substantial concerns with high-frequency transmission, such as enormous free-space path losses, massive losses because of obstacles, and practical difficulties, particularly with power amplification. Adopting LIS as a novel approach allows us to have a large number of small-sized antenna aggregates with a large number of panels [6]. In addition, the significant reflection effects in LIS can be used to increase coverage [7]. Using these qualities, we could develop communications with several orders of magnitude larger capacities than current wireless networks. In fact, new communications approaches such as LIS can be fully utilized to improve performance [8]. The LIS system can be viewed as an extension of m-MIMO, which can receive and transmit from a man-made structure. As a result, user terminals establish communications from a close distance, which reduces battery consumption and reduces interference [1,6]. The LIS system has better channel estimation capabilities than m-MIMO, which typically requires Channel State Information (CSI) for hundreds of antennas. In addition, the LIS system is reliable and efficient [9]. Four different receivers are studied in this article and compared in terms of performance: namely, Zero Forcing (ZF), Maximum Ratio Combining (MRC), Equal Gain Combining (EGC), and Minimum Mean Squared Error (MMSE) [6,10]. Moreover, low-density parity-check codes (LDPC) coding is studied in the scenario of the LIS system combined with SC-FDE transmission, leading to a reduction in the Bit Error Rate (BER) [11,12]. The integration of LDPC in the scenario of the LIS system combined with SC-FDE transmission is the novelty of the article.

LDPC codes are particularly efficient because they provide a feasible implementation that approaches the Shannon channel capacity for reliable transmission. LDPC codes are critical for many current communication systems due to their capacity-approaching performance and low-complexity iterative decoding over noisy information channels [13]. LDPC codes outperform other error-correcting codes in many respects, including how well they manage errors and how cheap it is to encode and decode them. QC-LDPC (Quasi-Cyclic LDPC) codes, also known as architecture-aware codes, are a particularly important type of algebraically constructed LDPC code that was introduced in 2005 [14,15]. They are included in a number of communication system standards, including IEEE 802.16 e, DVB-S2, and 802.11. QC-LDPC codes are built using finite geometries or circulant permutation matrices. This is because their parity check matrices have a unique shape that makes it easier to build a hardware encoder and decoder [14].

1.2. Structure of LDPC Code

The sparse parity check matrix can be used in LDPC code to define parity check sets. The term "Sparse" in a matrix with the $(n - k) \times n$ dimension denotes that there are fewer instances of "1" than there are of "0". There are more zeros than ones in $(n - k) \times n$ entries. The sparse parity check matrix, (n, w_c, w_r) , is defined by three variables. n stands for the coded length, while w_r and w_c represent the number of ones in a row and a column, respectively. The w_c and $w_r \ll n \times (n - k)$ requirements must be met for a matrix to be referred to as low-density or sparse [15].

Parity Check Matrix can be classified into two types: Regular and Irregular. Moreover, LDPC codes can be encoded and decoded using a variety of methods. The common objective of all systems is to simplify and speed up the encoding and decoding process. Linear Block Code (n, k) is the foundation for the encoding method that is used most frequently. The message bits and parity bits that make up a Linear Block Code codeword can be described as follows: m is the message, and p is the parity vector.

According to Linear Block Code's characteristics, $C \cdot H^T = 0$. We obtain the equations for $P_{n-k \times 1}$ in terms of message bits to satisfy this criterion via matrix multiplication. Therefore, after obtaining the values of $P_{n-k \times 1}$, we may obtain the N-bit codeword.

The bit-flipping algorithm and the sum-product method are used to decode LDPC codes. There are two categories of decoding: hard decision decoding and soft decision decoding. Decoding by bit-flipping corresponds to a hard-decision message-passing algorithm [16].

A list of acronyms used in this paper is provided in Table 1.

Table 1. A list of acronyms.

Acronym	Description
AWGN	Additive White Gaussian Noise
BER	Bit Error Rate
BS	Base Station
CSI	Channel State Information
CP	Cyclic Prefix
DFT	Discrete Fourier Transform
EGC	Equal Gain Combining
IB-DFE	Iterative Block Decision Feedback Equalization
ELAA	Extremely Large Antenna Arrays
IB-DFE	Iterative Block—Decision Feedback Equalization
IDFT	Inverse DFT
IoT	Internet of Things
IRS	Intelligent Reflecting Surface
LDPC	Low-Density Parity-Check
LIS	Large Intelligent Surface
m-MIMO	Massive Multiple-Input Multiple-Output
MFB	Matched Filter Bound
MIMO	Multiple-Input Multiple-Output
MRC	Maximum Ratio Combining
MMSE	Minimum Mean Squared Error
OFDM	Orthogonal Frequency Division Multiplexing
QC-LDPC	Quasi Cyclic—Low Density Parity Check
QoS	Quality of Service
SC-FDE	Single Carrier with Frequency Domain Equalization
UE	User Equipment
UM-MIMO	Ultra Massive Multiple-Input Multiple-Output
ZF	Zero Forcing

1.3. Objective, Contribution, and Organization

Previous work considered using the block transmission techniques Orthogonal Frequency Division Multiplexing (OFDM) and SC-FDE and their combination in MIMO or LIS systems [17–19]. The research published in [18] studies the performance of LDPC-Coded m-MIMO associated with non-orthogonal multiple access techniques. The novelty of this article relies on studying the performance of the LIS system with LDPC codes and SC-FDE transmission.

This article is divided as follows: Section 2 details system and signal characterization; Section 3 analyses performance outcomes; Section 4 summarizes this article; and Section 5 presents future research.

2. System and Signal Characterization

It is known that OFDM presents a high Peak-to-Average Power Ratio (PAPR), which tends to be problematic in the uplink scenario (i.e., transmission from the user terminal to the base station) [9,16]. In such a scenario, SC-FDE transmission presents a lower significant PAPR than OFDM signals. This is an important advantage because it allows for more efficient power amplification, which is critical in terminals [9].

The LIS system behaves as a near-field beamformer, meaning that communication takes place beyond the Fraunhofer distance. It has the following characteristics [2]:

- While MIMO systems have an antenna element separation of 3λ to 4λ , the LIS has an antenna element spacing typical of $\lambda/2$.

- Far-field wireless communications are typically established at propagation distances greater than the Fraunhofer distance (the Fraunhofer distance is only a few wavelengths).
- Individual elements of the LIS array can be seen in the far field, but the whole array, which acts in the short field, cannot be seen.
- Therefore, the focus is set on the distance, the bearing, and the elevation planes. This acts similar to a lens to focus the sun’s energy on a piece of paper. Note that traditional beamforming does not focus on distance, but only on bearing and elevation.
- LIS is different from traditional beamforming in that it can suppress the interference between users that are aligned, in terms of bearing and elevation, but at different ranges. This makes the process of concentrating energy even better.

Various reception topologies are taken into consideration for SC-FDE signals, including the widely used ZF and MMSE receivers and lower-complexity receivers such as the MRC or the EGC. The levels of complexity of MRC and EGC are lower than ZF and MMSE because the latter receivers require the inversion of the channel matrix for each frequency component, while the former does not require this processing [17,18]. Note that such matrix inversion is highly demanded from the point of view of processing and, consequently, energy consumption. For the MRC and EGC, consisting of non-optimum receivers having some level of interference generated in the decoding processing, they can be combined with iterative interference cancellation schemes to reduce the inherent residual interference levels. Iterative block decision feedback equalization (IB-DFE) is another type of receiver that is often used in SC-FDE systems [5,19].

As depicted in Figure 1, the n th transmitted block, of N data symbols, sent by the t th UE is denoted as $s_n^{(t)}$, while the received block by the r th antenna of the LIS system is denoted as $y_n^{(r)}$. Note that the communication between the UE and the LIS system is established in the near-field, instead of far-field. The mapping between the time domain signal and the frequency domain signal, for the k th subcarrier (assumed invariant during the transmission of a given block), of the transmitted block is defined as $DFT\{s_n^{(t)}; n = 0, 1, \dots, N - 1\} = \{S_k^{(t)}; k = 0, 1, \dots, N - 1\}$, i.e., by performing the Discrete Fourier Transform (DFT) of the time-domain block. Similar mapping is assumed for the received block as $DFT\{y_n^{(r)}; k = 0, 1, \dots, N - 1\} = \{Y_k^{(r)}; k = 0, 1, \dots, N - 1\}$.

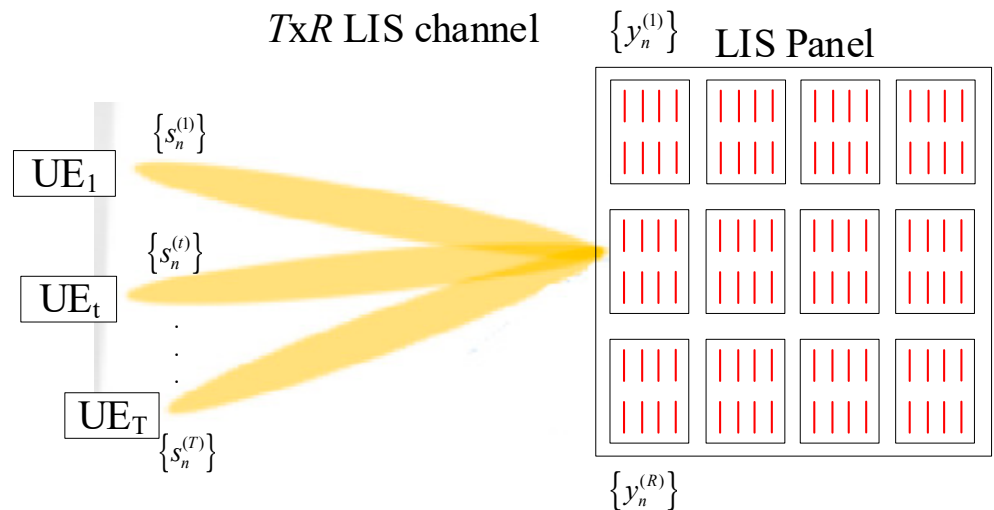


Figure 1. Block diagram of an LIS System.

After removing the cyclic prefix, and assuming a cyclic prefix longer than the overall channel impulse response of each channel, using the matrix-vector representation, we arrive at the received frequency-domain signal [20]:

$$Y_k = [Y_k^{(1)}, \dots, Y_k^{(R)}] = H_k S_k + N_k \tag{1}$$

where $S_k = [S_k^{(1)}, \dots, S_k^{(T)}]^T$ stands for the frequency domain transmitted data symbols; where H_k denotes the $T \times R$ channel matrix for the k th subcarrier, with (r, t) th element $H_k^{(t,r)}$; and where H_k denotes the channel frequency response for the k th subcarrier (assumed invariant during the transmission of a given block). Note that the mapping between the time and frequency domains is defined by $\{H_k; k = 0, 1, \dots, N - 1\} = DFT\{h_n; n = 0, 1, \dots, N - 1\}$. Moreover, N_k is the frequency-domain block channel noise for that subcarrier [21].

3. System and Signal Model for the Receivers

In LIS systems scenarios, various receiver design strategies are possible. First, linear feedforward non-iterative FDE receivers such as ZF, MMSE, MRC, and EGC, and second, nonlinear feedback equalization iterative MRC and EGC receivers are possible (Figure 2).

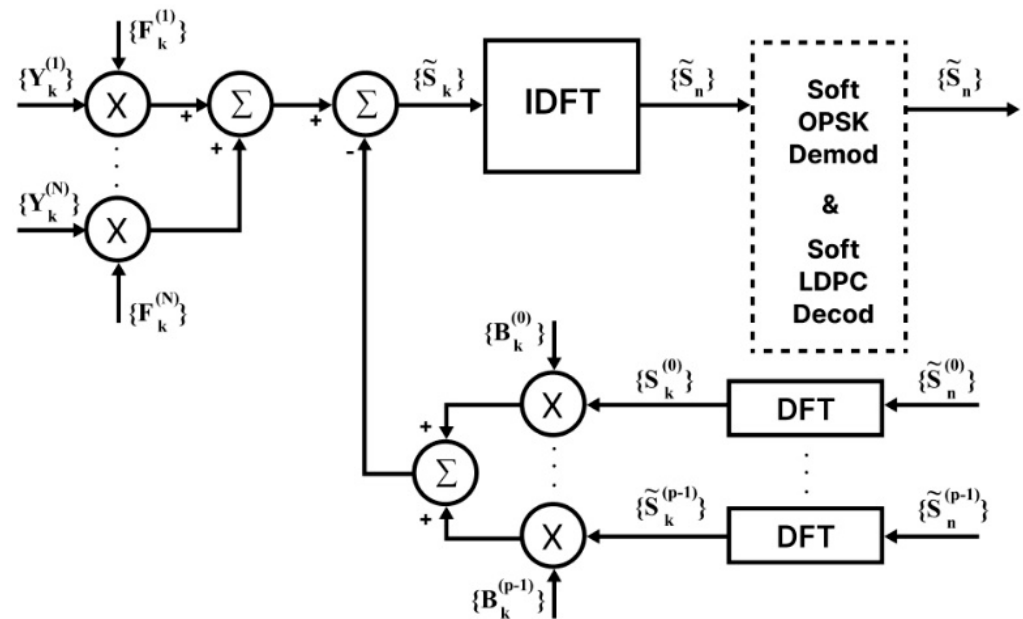


Figure 2. Block diagram using SC-FDE receiver.

Although their BER results can be excellent, the ZF and MMSE algorithms, which are based on matrix inversions, are plainly detrimental in this sort of system since the computational cost increases dramatically with the number of transmitting and receiving antennas. Contrarily, the MRC and EGC procedures are simple, leading to a decrease in processing and, consequently, energy saving.

Assuming a non-iterative receiver, the estimated frequency domain data symbols

$$\tilde{S}_k = [S_k^{(1)}, \dots, S_k^{(R)}]^T \text{ is:}$$

$$\tilde{S}_k = F_k Y_k \tag{2}$$

Depending on the algorithm, F_k , the detection coefficient corresponding to the k th subcarrier, can be computed [20] as:

$$F_k = \frac{1}{H_k} \tag{3}$$

For the evaluation of these different receivers, we need information about the feed-forward and feedback matrices where F_k denotes feedforward and B_k shows feedback matrices, respectively.

3.1. Linear Feedforward Non-Iterative FDE Receivers

3.1.1. Zero Forcing

The signals of each transmitting antenna are considered the target signal by the ZF receiver, while the other outputs are considered interferers. The main job of this receiver is to reduce the interference to zero by inverting the channel response and fitting the result to the closest letter in the alphabet being looked at. The inverse channel, H^{-1} , is then multiplied by the received signal, Y_k , as described above.

The ZF criterion considerably increases the channel noise in sub-channels with local deep notches during the channel equalization process. Using the ZF algorithm, F_k becomes [10]:

$$F_k = \left(H_k^H H_k \right)^{-1} H_k^H \tag{4}$$

3.1.2. Minimum Mean Squared Error

The IDFT (Inverse DFT) of the block \bar{S}_k , with $k = 0, 1, \dots, N - 1$ can be used to determine the data symbols for a linear MMSE-based receiver [17]:

$$\bar{S}_k = \left[S_{k(1)}, \dots, S_{k(R)} \right]^T = \left(H_k H_k^H + \beta I \right)^{-1} H_k^H Y_k \tag{5}$$

where

$$\beta = \frac{\sigma_N^2}{\sigma_S^2} = \frac{\frac{E[|N_k|^2]}{2}}{\frac{E[|S_k|^2]}{2}} \tag{6}$$

with regard to (3,4):

$$F_k = \left(H_k H_k^H + \beta I \right)^{-1} H_k^H \tag{7}$$

where I stands for the identity matrix. For all the contents of transmitter and receiver, β is taken to be the same. However, in LIS systems, the sizes of these matrices can be enormous, which imposes great requirements to perform the inversion of the channel matrix for each channel frequency response component.

3.1.3. Maximum Ratio Combining

It is proposed to use sub-optimal equalization techniques that do not require channel matrices' inversions and are thus easier to implement. Maximum ratio detection has the best performance of all the combining schemes because the set of possible combining vectors is not limited. Less complicated receivers are often used in massive MIMO systems, being also well suited for LIS systems. Undoubtedly, the ones constructed using the MRC [21] are the most well liked.

Using the MRC algorithm, F_k becomes:

$$F_k = H_k^H \tag{8}$$

3.1.4. Equal Gain Combining

It has been demonstrated that Equal-Gain detection receivers perform generically well in terms of average error probability of symbol [22]. Simple hardware complexity is all that is expected for Equal Gain Combiners at the i th receiving antenna. Equalization is performed at the receiver by dividing the received symbol y_i by phase h_i . This is represented by the polar form $h_i e^{j\theta}$ of the channel h_i .

The total number of phase-compensated channels received by all antennas makes up the encoded symbols [23]. Using the EGC algorithm, F_k becomes:

$$F_k = e^{j * \text{Arg}(H_k^H)} \tag{9}$$

3.2. Iterative MRC and EGC FDE Receivers (IB-DFE Receivers)

It is known that the MRC and EGC receivers are sub-optimal, and their performance normally improves by adopting an iterative approach. In IB-DFE receivers, for a given i th iteration (see Figure 3), the output samples are given by [5,17]:

$$\tilde{S}_k^{(i)} = \sum F_k^{(l,i)} Y_k^{(l)} - B_k^{(i)} \hat{S}_k^{(i-1)} \tag{10}$$

where $\hat{S}_k^{(i-1)}$ is the DFT of the $(i - 1)$ th iteration’s hard-decision block $\hat{s}_n^{(i-1)}$, which is associated with the transmitted time-domain block s_n .

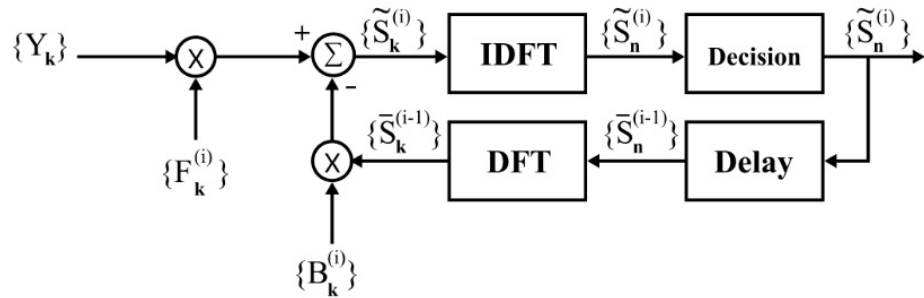


Figure 3. Block diagram of IB-DFE receivers.

Moreover,

$$\tilde{s}_n^{(i)} = \gamma^{(i)} \cdot s_n + \varepsilon_n^{eq(i)} \tag{11}$$

where $\varepsilon_n^{eq(i)}$, represents the overall error, which includes both channel noise and residual intersymbol interference, and

$$\gamma^{(i)} = \frac{1}{N} \sum_{k=0}^{N-1} \sum_{l=1}^L F_k^{(l,i)} H_k^{(l)} \tag{12}$$

From [10,15], it is shown that the optimum feedforward and feedback coefficients are given by:

$$F_k^{(l,i)} = \frac{H_k^{(l)*}}{\beta + (1 - (\rho^{(i-1)})^2) \sum_{l'=1}^L |H_k^{(l')}|^2} \tag{13}$$

$$B_k^{(i)} = \rho^{(i-1)} \left(\sum_{l'=1}^L F_k^{(l',i)} H_k^{(l')} - 1 \right), \tag{14}$$

with

$$\rho^{(i)} = \frac{E \left[s_n^* s_n^{(i)} \right]}{E \left[|s_n|^2 \right]} \tag{15}$$

Based on the characteristics of each frequency, we could use MRC or EGC to perform frequency-domain processing on SC-FDE signals. The residual interference levels, however, can still be significant, particularly for modest values of T/R. The iterative interference canceller (receiver) shown in Figure 3 suggests as a solution to use the following process:

$$\tilde{S}_k = Y_k - C_k \bar{S}_k, \tag{16}$$

where C_k defines the interference cancellation matrix, defined as [24]

$$C_k = H_k B_k - I, \tag{17}$$

and where I stands for an $R \times R$ identity matrix.

4. Simulation Results and Analysis

This section studies the BER performance results obtained with Monte Carlo simulations, using LIS systems, in the uplink direction, associated with SC-FDE block transmission technique and LDPC codes. E_b stands for the energy of the transmitted bits, and N_0 is the one-sided power spectral density of the noise. The BER is calculated as a function of E_b/N_0 . A block size of $N = 256$ symbols was used for the QPSK modulation (identical results were seen for different values of N , given that $N \gg 1$). With a code rate of $\frac{1}{2}$, LDPC codes 32,400 long were considered in the simulations.

The LIS system comprises several panels, whereas each panel includes several antenna elements. The distance between the antenna elements is $\lambda/2$. The channel correlation between the antenna elements allows for the creation of the above-described beam. Five statistically independent equal power paths were considered in the Monte Carlo simulation to translate for an extreme Rayleigh fading channel.

The simulations considered four receiver types: ZF, MMSE, MRC, and EGC. The following graphics include, in some cases, results with and without equalization for the MRC and EGC receivers, while ZF and MMSE receivers cannot avoid equalization. This makes MRC and EGC even simpler, besides the possibility of avoiding the channel matrix inversion for each frequency component of the channel.

Except for ZF, all other receivers did not consider equalization (and iterations were not considered). Comparing these not-equalized receivers with iterative receivers that include equalization (in this case, we took into account the repetitive receivers in four iterations), the results are the same, as equalization does not bring any added value when the number of antennas is sufficiently high, which is the generic case of the LIS system. It is worth noting that the other receivers do not compute the channel matrix inverse for each frequency component, whereas the ZF does [25]. This makes the ZF significantly more computationally intensive.

For comparison purposes, the Matched Filter Bounds (MFB) curves are considered in different performance graphics, representing lower bounds. In general, the MFB for a frequency selective channel (i.e., a channel with Inter-Symbol Interference) is the performance when a single symbol is transmitted, which means there is no ISI-related degradation, experiencing only fading-related degradation. This can be regarded as a lower bound on the performance of a given receiver, although in many cases even an ideal equalizer (for instance, for a Viterbi equalizer) cannot achieve the MFB. This means that a receiver whose performance is a fraction of dB from the MFB will be close to an optimum receiver.

Table 2 presents a list of baseline simulations utilized in the different graphics of this section.

Figure 4 shows the performance results for 4X25 LIS system (four panels, each with 25 antennas, making a total of 200 antennas), with five users, without LDPC codes, with and without equalization, for the ZF, MRC, EGC, and MMSE, four distinct receivers. Note that only the MRC and EGC may avoid equalization, while ZF and MMSE receivers cannot get rid of this. This makes MRC and EGC even simpler, besides the possibility of avoiding the channel matrix inversion for each frequency component of the channel. As can be seen, for the MRC and EGC receivers and 4X25 LIS system, the equalization does not bring any added value in terms of performance improvement, as compared to the results without equalization. Moreover, in this scenario, channel estimation is not required. From these results, we can conclude that the LIS system allows the use of very simple processing, as equalization and channel estimation are avoided, at least for this LIS configuration. Moreover, the MMSE and ZF are the receivers that achieve the best performance, and their curves are almost superimposed. On the other hand, the MRC performs better than the EGC (whose performance is the worst), but these receivers present a high level of simplicity.

Table 2. The baselines used in Monte Carlo simulations.

Figure	Number of Antennas per Four Panels	Number of Users (Including the Reference User)	Equalization	Selective LIS	Number of Antennas Used in Selective LIS	LDPC	Objective
Figure 4	25	5	With and without	No	-	No	Absence of performance improvement with the use of equalization
Figure 5	225	5	With and without	No	-	No	Absence of performance improvement with the use of equalization
Figure 6	25 versus 225	2	Without	No	-	No	Performance of 4X25 versus 4X225 LIS system
Figure 7	25	2, 5 and 10	Without	No	-	No	Loss of performance that occurred with the increase of the number of users
Figure 8	25	5	Without	No	-	Yes and No	Performance improvement with LDPC codes, compared to the uncoded system, for 4X25
Figure 9	225	5	Without	No	-	Yes and No	Performance improvement with LDPC codes, compared to the uncoded system, for 4X225
Figure 10	225	5	Without	Yes and No	20 and 100	No	Performance degradation using Selective LIS, varying the number of antennas

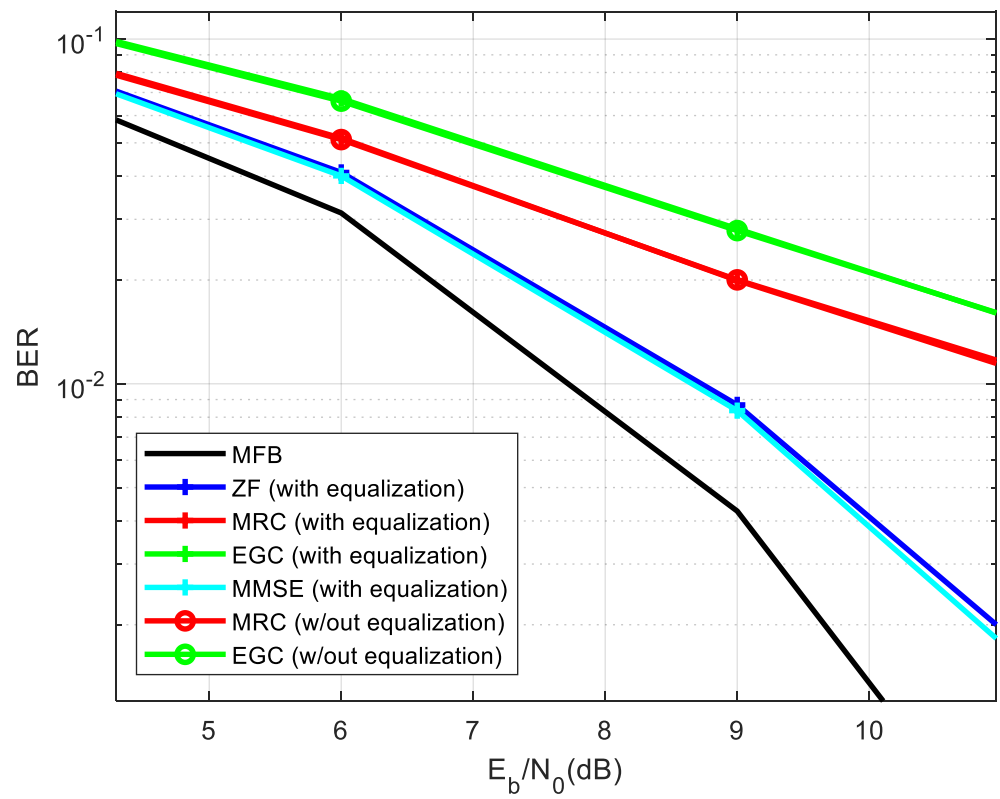


Figure 4. Results for 4X25 LIS System, with 5 users, without LDPC codes, with and without equalization.

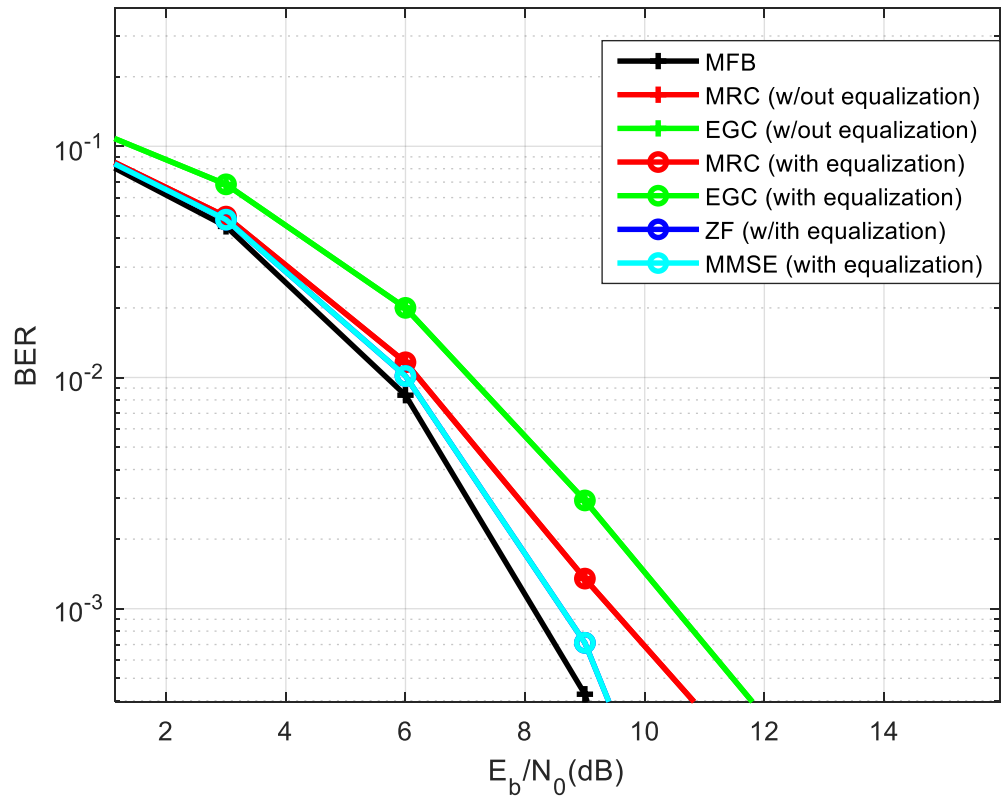


Figure 5. Results for 4X225 LIS System, with 5 users, without LDPC codes, with and without equalization.

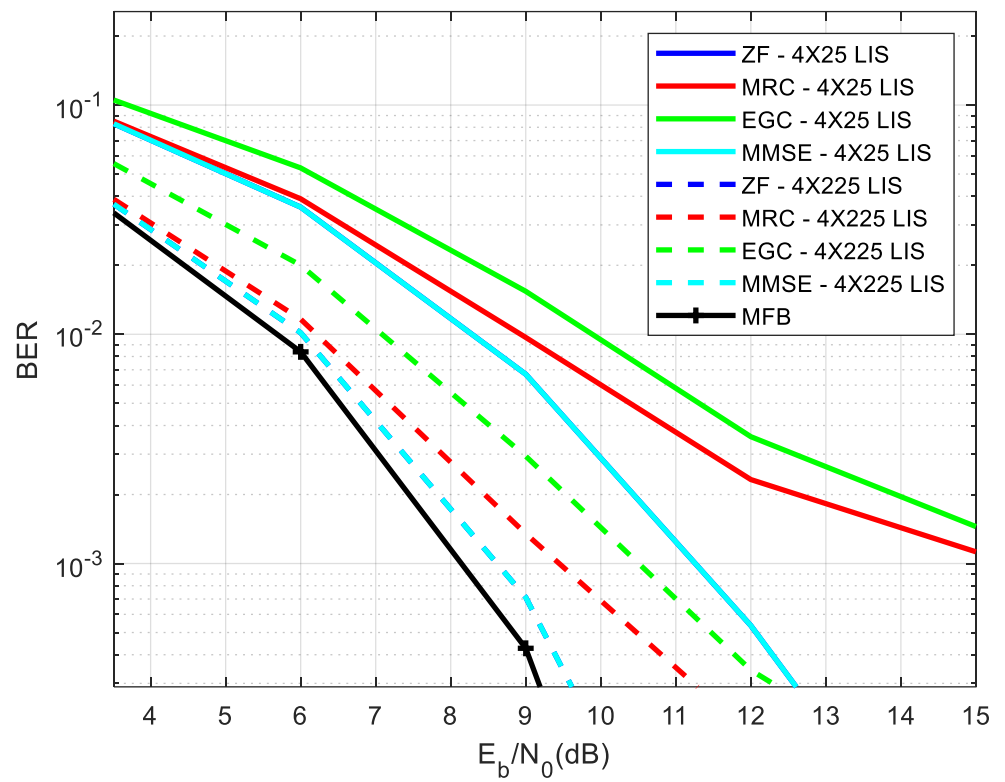


Figure 6. Results for 4X25 versus 4X225 LIS System, with 2 users, without LDPC codes.

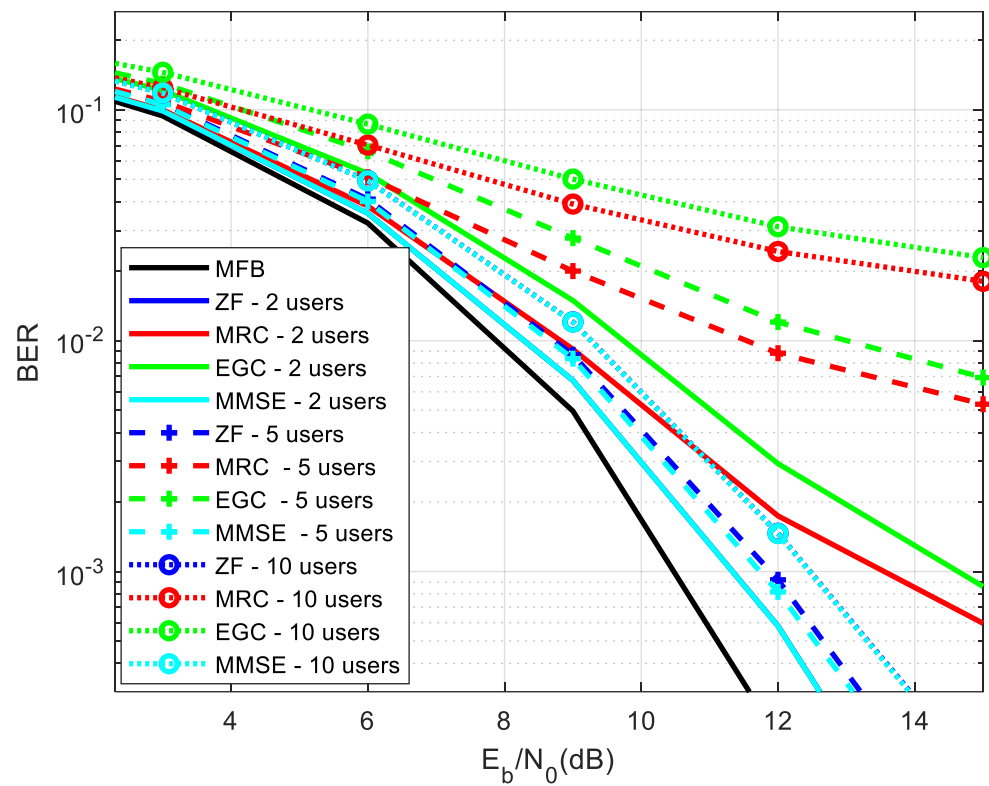


Figure 7. Results for 4X25 LIS System, with 2, 5, and 10 users, without LDPC codes.

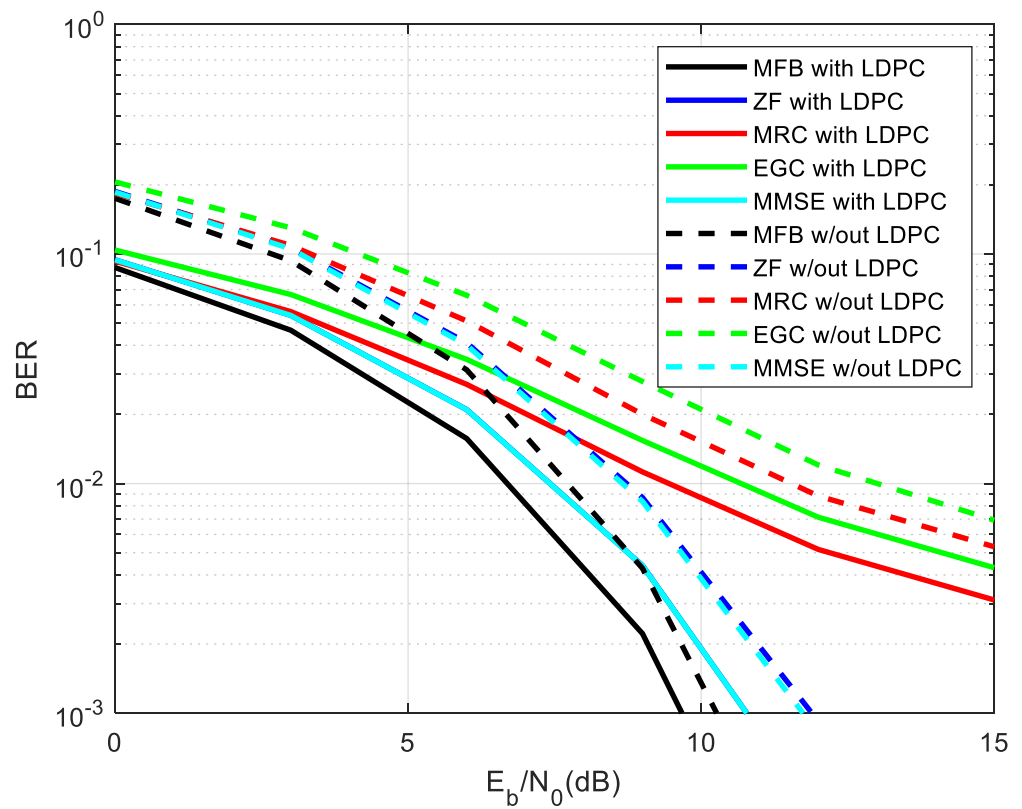


Figure 8. Results for 4X25 LIS System, with 5 users, with and without LDPC codes.

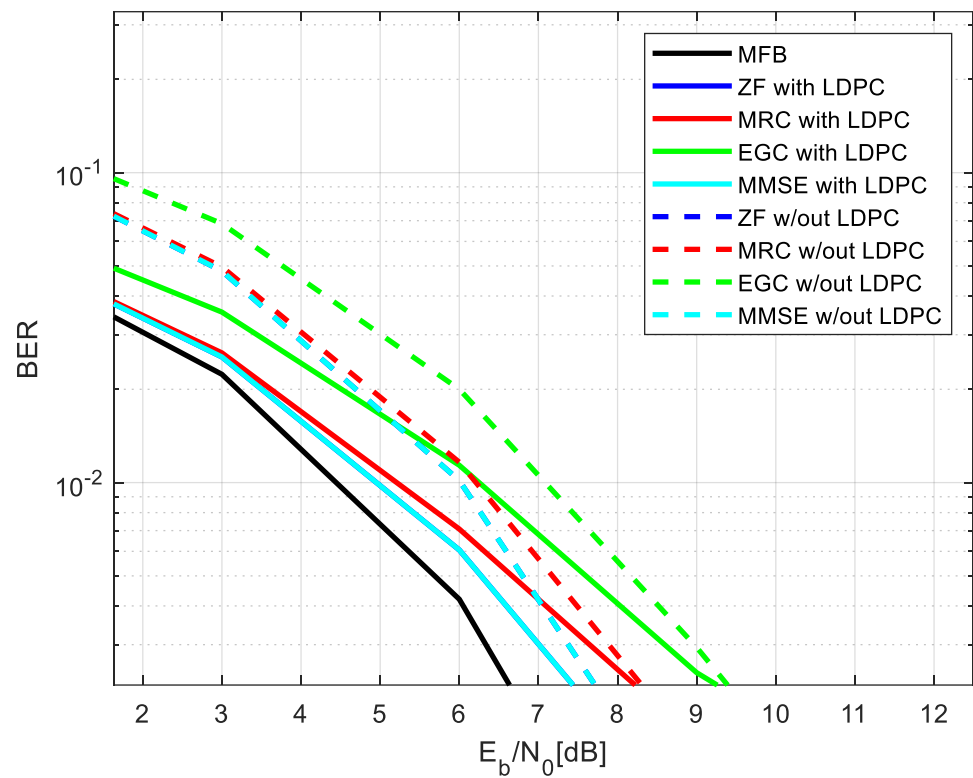


Figure 9. Results for 4X225 LIS System, with 5 users, with and without LDPC codes.

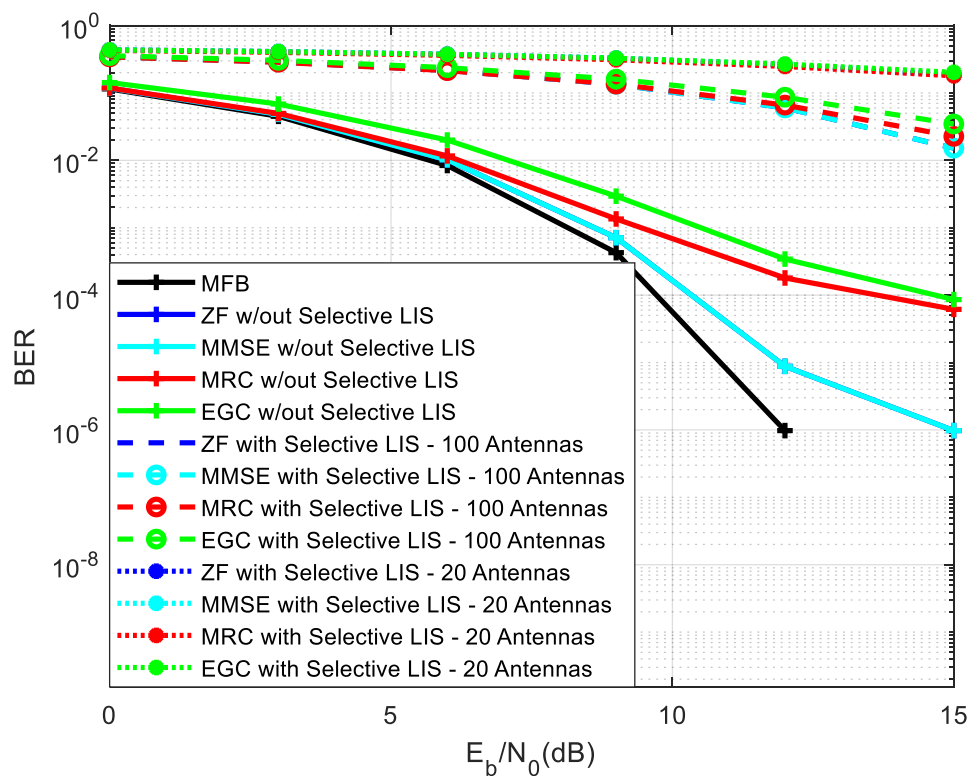


Figure 10. Results for 4X225 LIS System, with 5 users, without Selective LIS versus with Selective LIS (20 versus 100 antennas).

Figure 5 displays the effectiveness outcomes for 4X225 LIS system (four panels, each with 225 antennas, making a total of 900 antennas), with five users, without LDPC codes, with and without equalization. Similar to the results with 4X25 LIS system, and for the MRC and EGC receivers, the use of equalization does not bring any added value in terms of performance improvement. Moreover, the ZF and MMSE are those receivers that are closer to the MFB, whose curves are superimposed, while the EGC is the one that performs worst. Comparing the results of 4X25 LIS System against 4X225 LIS System, one can conclude that the latter achieves better performance, and the difference of performance between different receivers is minimized. Similar to this graphic, note that the MMSE curves superimpose the ZF ones, in the remaining graphics.

Figure 6 shows the performance results 4X25 versus 4X225 LIS System, with two users (one reference user plus one interfering user), for four distinct receivers: the ZF, MRC, EGC, and MMSE, without LDPC codes. As before, the MMSE curve superimposes the ZF one. For all receiver types, the efficiency-obtained results with the 4X225 LIS system are better than those achieved with the 4X25 LIS system, as indicated. Nevertheless, it should be mentioned that the MRC, EGC, and MMSE are less computationally demanding than the ZF. Finally, it should be mentioned that the EGC achieves the worst performance.

Figure 7 displays the operational outcomes for the 4X25 LIS System with two, five, and 10 users, without LDPC codes. As expected, increasing the number of users results in a decrease of performance. Nevertheless, it is observed that the degradation of performance is moderate for the MMSE and ZF receivers, being more visible for the MRC and EGC receiver types.

Figure 8 displays the operational outcomes for 4X25 LIS System, with five users, with and without LDPC codes. With regard to these outcomes, we observe that the use of LDPC codes results in a performance improvement of the order of 3 dB, for all receiver types.

Figure 9 displays the results of the effort for 4X225 LIS System, with five users, with and without LDPC codes. Similar to the results of Figure 8, we find that applying LDPC

codes resulted in an optimisation of performance of the order of 2 dB over a comparable uncoded scheme.

Figure 10 displays the results of the effort for 4X225 LIS System, with five users, without Selective LIS versus with Selective LIS (20 and 100 antennas). Selective LIS corresponds to using a subset of the total number of antennas. The algorithm employed in the selective LIS corresponds to those antennas that are placed at shorter distance from the mobile terminal. As expected, the use of selective LIS results in a performance degradation relating to the system without selective LIS. Moreover, decreasing the number of antennas considered by the selective LIS also translates in a degradation of performance.

5. Conclusions

This article presents a performance analysis of a LIS system, with and without LDPC coding, associated to the SC-FDE transmission, and using four different types of receivers: ZF, MMSE, MRC, and EGC.

It was seen that one of the advantages of the LIS System relies on its improved performance, facilitating simplicity as well, namely due to the possibility of not using equalization. It was also seen that by increasing the number of the antennas that form the LIS, the performance improves, regardless whether LDPC codes are used or not.

The ZF and MMSE are the receivers that perform closer to the MFB, whose performance curves are almost superimposed, while the EGC is the one that performs worst. It is worth noting that the ZF and MMSE receivers are more complex because, for each frequency component, the computation of the inverse channel matrix is required.

It was seen that the MRC and EGC receivers may be used without equalization, without degrading the performance, while ZF and MMSE receivers cannot avoid equalization. This makes MRC and EGC even simpler, besides the possibility of avoiding the channel matrix inversion for each frequency component of the channel. Moreover, in this scenario, channel estimation is not required, which also facilitates the system.

Finally, it was demonstrated that a system comprising LIS, associated with LDPC codes, and coupled with the SC-FDE transmission technique, exhibits performance optimization that improves with increased number of antennas. The MMSE receiver achieves the best overall performance, but this is achieved at the cost of a more computational demanding system, and where equalization cannot be avoided. When low complexity is a requirement, avoiding channel matrix inversion, equalization, and channel estimation, the MRC receiver is a good option to make cellular communications better in the future.

6. Future Research

Future research will extend the current work to Intelligent Reflecting Surface (IRS), as an extension to the LIS, as well as to OFDM transmission.

Author Contributions: All authors contributed equally to the article. All authors have read and agreed to the published version of the manuscript.

Funding: This work is funded by FCT/MCTES through national funds and, when applicable, co-funded EU funds under the projects UIDB/EEA/50008/2020 and 2022.03897. PTDC.

Institutional Review Board Statement: Not applicable.

Informed Consent Statement: Not applicable.

Data Availability Statement: Data was obtained using Monte Carlo simulations and implemented using Matlab.

Acknowledgments: We acknowledge the support of FCT/MCTES, as described above in the funding section. We also acknowledge the support of Autonomia TechLab for providing an interesting environment in which to carry out this research.

Conflicts of Interest: The authors declare no conflict of interest.

References

1. Decarli, N.; Dardari, D. Communication Modes with Large Intelligent Surfaces in the Near Field. *IEEE Digit. Object Identifier* **2021**, *9*, 165648–165666. [[CrossRef](#)]
2. Bjornson, E.; Özlem, T.; Sanguinetti, L. A primer on near-field beamforming for arrays and reconfigurable intelligent surfaces. In Proceedings of the 2021 55th Asilomar Conference on Signals, Systems, and Computers (ACSSC), Pacific Grove, CA, USA, 31 October–3 November 2021; pp. 105–112.
3. Dajer, M.; Ma, Z.; Piazzzi, L.; Narayan, P.; Qi, X.; Sheen, B.; Yang, J.; Yue, G. Reconfigurable Intelligent Surface: Design the Channel—A New Opportunity for Future Wireless Networks. *arXiv* **2020**, arXiv:2010.07408v1. [[CrossRef](#)]
4. Borger, D.; Dinis, R.; Montezuma, P. An MRC-Based Receiver for SC_FDE Modulations with Massive MIMO Schemes. In Proceedings of the 2016 IEEE Global Conference on Signal and Information Processing (Global SIP), Washington, DC, USA, 7–9 December 2016.
5. Marques da Silva, M.; Dinis, R.; Guerriero, J. A Low Complexity Channel Estimation and Detection for Massive MIMO using SC-FDE. *Telecom* **2020**, *1*, 3–17. [[CrossRef](#)]
6. Pereira, A.; Rusek, F.; Gomes, M.; Dinis, R. On the Complexity Requirements of a Panel-Based Large Intelligent Surface. In Proceedings of the 2020 IEEE Global Communications Conference, Taipei, Taiwan, 7–11 December 2020.
7. Hu, S.; Rusek, F.; Edfors, O. Beyond Massive-MIMO: The Potential of Data-Transmission with Large Intelligent Surfaces. *arXiv* **2017**, arXiv:1707.02887v1. [[CrossRef](#)]
8. Sanchez, J.R.; Rusek, F.; Edfors, O.; Liang, L. Distributed and Scalable Uplink Processing for LIS: Algorithm, Architecture, and Design Trade-offs. *arXiv* **2020**, arXiv:2012.05296v1.
9. Wang, J.; Baykas, T.; Funada, R.; Sum, C.S.; Rahman, A.; Lan, Z.; Harada, H.; Kato, S. A SNR Mapping Scheme for ZF/MMSE Based SC-FDE Structured WPANs. In Proceedings of the VTC Spring 2009—IEEE 69th Vehicular Technology Conference, Barcelona, Spain, 26–29 April 2009.
10. Pereira, A.; Bento, P.; Gomes, M.; Dinis, R.; Silva, V. Complexity analysis of FDE receivers for massive MIMO block transmission systems. *IET Commun. Inst. Eng. Technol.* **2019**, *13*, 1762–1768. [[CrossRef](#)]
11. Wenling, B.; Daqiao, B.; Yue, X. Performance evaluation of MIMO SC-FDMA system with FDE recoveries. In Proceedings of the 2009 IEEE International Conference on Wireless Communications & Signal Processing, Nanjing, China, 13–15 November 2009. [[CrossRef](#)]
12. Hu, Y.; Wang, W.; Lin, Z.; Ding, M. Performance Analysis of Reconfigurable Intelligent Surface Assisted Wireless System with Low-Density Parity-Check Code. *IEEE Commun. Lett.* **2021**, *25*, 2879–2883. [[CrossRef](#)]
13. Wanda, T. A Study on Performance of LDPC Codes on Power Line Communications. In Proceedings of the 2004 IEEE International Conference on Communications (IEEE Cat. No.04CH37577), Paris, France, 20–24 June 2004.
14. Asif, M.; Zhou, W.; Ajmal, M.; Akhtar, Z.A.; Khan, N.A. A Construction of High-Performance Quasi cyclic LDPC Codes: A Combinatoric Design Approach. *Hindawi Wirel. Commun. Mob. Comput.* **2019**, *2019*, 7468792. [[CrossRef](#)]
15. Johnson, S. Introducing Low-Density Parity-Check Codes. *Univ. Newctle. Aust.* **2006**, *1*, 2006. [[CrossRef](#)]
16. Yi, F.; Bi, G.; Yong Liang, G.; Lau, F. A Survey on Photograph LDPC Codes and Their Applications. *IEEE Commun. Surv. Tutor.* **2015**, *17*, 1989–2016.
17. Gang, X.; Shalinee, K. Joint transmitter and receiver design with adaptive beamforming in MIMO SC-FDMA systems. In Proceedings of the 2011 IEEE International Conference on Acoustics, Speech and Signal Processing (ICASSP), Prague, Czech Republic, 22–27 May 2011.
18. Pan, Y.; Zhixiang, D. Channel Estimation for Wireless Communication Systems Aided By Large Intelligent Reflecting Surface. In Proceedings of the IEEE 2nd International Conference on Big Data, Artificial Intelligence and Internet of Things Engineering (ICBAIE 2021), Nanchang, China, 26–28 March 2021.
19. Henghao, L.; Yongkui, M. Low-Complexity Iterative Block Decision Feedback Equalization for SC-FDE System. In Proceedings of the IEEE Eighth International Conference on Instrumentation & Measurement, Computer, Communication and Control (IMCCC), Harbin, China, 19–21 July 2018.
20. Montezuma, P.; Borges, D.; Dinis, R. Low Complexity MRC and EGC Based Receivers for SC-FDE Modulations with Massive MIMO Schemes. In Proceedings of the IEEE Global Conference on Signal and Information Processing-Global SIP, Washington, DC, USA, 7–9 December 2016.
21. Chen, J.; Liang, Y.C.; Cheng, H.V.; Yu, W. Channel Estimation for Reconfigurable Intelligent Surface Aided Multi-User MIMO Systems. *arXiv* **2019**, arXiv:1912.03619v1. [[CrossRef](#)]
22. Long, R.; Liang, Y.C.; Pei, Y.; Larsson, G.E. Active Reconfigurable Intelligent Surface Aided Wireless Communications. *IEEE Trans. Wirel. Commun.* **2021**, *20*, 4962–4975. [[CrossRef](#)]
23. Simon, M.K.; Alouini, M.S. *Digital Communication over Fading Channels*; Wiley-IEEE Press: New York, NY, USA, 2005.
24. Edfors, O. Analysis of DFT-Based Channel Estimators for OFDM. *Wirel. Pers. Commun.* **2000**, *12*, 55–70. [[CrossRef](#)]
25. Torres, P.; Charrua, L.; Gusmao, A. On the Uplink Detection Performance in MU-MIMO Broadband Systems with a Large Number of BS Antennas. In Proceedings of the 18th International OFDM Workshop 2014, Essen, Germany, 27–28 August 2014.

Disclaimer/Publisher’s Note: The statements, opinions and data contained in all publications are solely those of the individual author(s) and contributor(s) and not of MDPI and/or the editor(s). MDPI and/or the editor(s) disclaim responsibility for any injury to people or property resulting from any ideas, methods, instructions or products referred to in the content.